

Dentomaxillofacial Radiology

Evaluation of Temporomandibular Joint Osseous Degenerative Changes with Artificial Intelligence Generated STL Segmentations

--Manuscript Draft--

Manuscript Number:	DMFR-D-23-00141
Full Title:	Evaluation of Temporomandibular Joint Osseous Degenerative Changes with Artificial Intelligence Generated STL Segmentations
Short Title:	Evaluation of TMJ Degenerative Changes with AI-Generated STL Files
Article Type:	Research Article
Keywords:	temporomandibular joint; mandibular condyle; stereolithography; cone-beam computed tomography; artificial intelligence
Corresponding Author:	Kaan Orhan, DDS PhD Ankara Universitesi Ankara, --- Select One --- TURKEY
Corresponding Author Secondary Information:	
Corresponding Author's Institution:	Ankara Universitesi
Corresponding Author's Secondary Institution:	
First Author:	Kaan Orhan, DDS, PhD
First Author Secondary Information:	
Order of Authors:	Kaan Orhan, DDS, PhD Alex Sanders Gürkan Ünsal, DDS, PhD Matvey Ezhov Melis Mısırlı, DDS, PhD Maxim Gusarev Murat İçen, DDS, PhD Mamat Shamshiev Gaye Keser, DDS, PhD Maria Golitsyna Merve Önder David Manulis Cemal Atakan
Order of Authors Secondary Information:	
Manuscript Region of Origin:	TURKEY
Abstract:	<p>Objectives; This study aims to evaluate the reliability of AI-generated STL files in diagnosing temporomandibular joint (TMJ) pathologies and compare them to a "ground truth" diagnosis made by six radiologists. The study also examines the accuracy of STL files in detecting condyle-related pathologies. Methods; A total of 432 retrospective CBCT images from four universities were evaluated by six dentomaxillofacial radiologists who identified pathologies such as flattening, erosion, osteophyte formation, bifid condyle formation, and osteosclerosis. Following the first evaluation stage, a consensus meeting was held to create a ground truth diagnosis, which was compared to AI-generated STL files using a web-based dental AI software.</p>

	<p>The interclass correlation (ICC) value was calculated for each pathology. Results; The ground truth diagnosis identified 372 cases of flattening, 185 cases of erosion, 70 cases of osteophyte formation, 117 cases of osteosclerosis, and 15 cases of bifid condyle formation out of 864 condyles. The ICC values for flattening, erosion, osteophyte formation, osteosclerosis, and bifid condyle formation were 1.000, 0.782, 1.000, 0.000, and 1.000, respectively, when comparing diagnoses made with STL files to the ground truth. Conclusions; AI-generated STL files are reliable for diagnosing bifid condyle formation, osteophyte formation, and flattening of the condyle. However, the diagnosis of osteosclerosis using AI-generated STL files is not reliable, and erosion grade affects the accuracy of diagnosis.</p>
Suggested Reviewers:	

Evaluation of Temporomandibular Joint Osseous Degenerative Changes with Artificial Intelligence-Generated STL Files

Abstract

Objectives; This study aims to evaluate the reliability of AI-generated STL files in diagnosing temporomandibular joint (TMJ) pathologies and compare them to a "ground truth" diagnosis made by six radiologists. The study also examines the accuracy of STL files in detecting condyle-related pathologies. **Methods;** A total of 432 retrospective CBCT images from four universities were evaluated by six dentomaxillofacial radiologists who identified pathologies such as flattening, erosion, osteophyte formation, bifid condyle formation, and osteosclerosis. Following the first evaluation stage, a consensus meeting was held to create a ground truth diagnosis, which was compared to AI-generated STL files using a web-based dental AI software. The interclass correlation (ICC) value was calculated for each pathology. **Results;** The ground truth diagnosis identified 372 cases of flattening, 185 cases of erosion, 70 cases of osteophyte formation, 117 cases of osteosclerosis, and 15 cases of bifid condyle formation out of 864 condyles. The ICC values for flattening, erosion, osteophyte formation, osteosclerosis, and bifid condyle formation were 1.000, 0.782, 1.000, 0.000, and 1.000, respectively, when comparing diagnoses made with STL files to the ground truth. **Conclusions;** AI-generated STL files are reliable for diagnosing bifid condyle formation, osteophyte formation, and flattening of the condyle. However, the diagnosis of osteosclerosis using AI-generated STL files is not reliable, and erosion grade affects the accuracy of diagnosis.

Keywords: temporomandibular joint; mandibular condyle; stereolithography; cone-beam computed tomography; artificial intelligence

1. INTRODUCTION

1.1. Temporomandibular Joint Anatomy

The Temporomandibular Joint (TMJ), which is localized between the condylar process of the mandible and the articular eminence of the temporal bone, allows the masticatory functions and phonation while adding mobility features to the skull.^{1, 2, 3, 4} TMJ is localized bilaterally, on each side of the skull, and shares similar features with the other mobile joints, such as an articular capsule, a synovial membrane, ligaments, an articular disc, and bony surfaces.^{4, 5, 6, 7} The articular surfaces of the TMJ differ from other joints in that the TMJ is covered by fibrocartilage instead of hyaline cartilage.^{1, 4, 6, 8, 9}

The most important bony landmark for the mandible is the mandibular condylar process, and the condyle has both lateral and medial poles, which gives it the bipolar characteristic structure.^{2, 3, 6, 8, 10, 11} It was reported that TMJ osteoarthritis was found in 13% of elder patients at radiographic levels; however, an autopsy study showed that 28% of the TMJ bony structures in a younger group and 50% in an older group were affected by degenerative changes.¹²

As the osteoarthritis diagnosis of TMJ depends on the clinical and radiographic examination findings, cone-beam computed tomography (CBCT) and MDCT (multi-detector computed tomography) are superior to magnetic resonance imaging (MRI) for the evaluation of the osseous changes.^{1, 2, 5, 6, 8, 10} Although Hintze et al. found no significant differences in the detection of morphological changes between CBCT and MDCT, the lower radiation dose makes CBCT preferable for diagnosis.^{12, 13}

1 The common morphological deformities and osseous changes that can be analyzed by CBCT
2 are the following:^{2, 4, 5, 6, 7, 12}

- 3 • Flattening of the TMJ condyle surface
- 4 • Erosion of the TMJ Condyle
- 5 • Bifid Condyle Formation
- 6 • Osteophyte Formation on the TMJ Condyle
- 7 • Osteosclerosis of the TMJ condyle
- 8 • Hyperplasia of the TMJ condyle
- 9 • Hypoplasia of the TMJ condyle

10 11 12 13 **1.2. TMJ and CBCT**

14
15 Following the study results of the SEDENTEX-CT project¹⁴, the use of CBCT for the
16 dentomaxillofacial area has been addressed by the European Academy of Dentomaxillofacial
17 Radiology (EADMFR) as "Basic Principles for Use of Dental Cone-Beam CT. Consensus
18 Guidelines of the EADMFR" in 2009, and according to the suggestions of the EADMFR's
19 guideline, the evaluation of developmental anomalies, traumas, osteoarthritis, ankylosis CBCT
20 has numerous advantages compared to other 3D imaging modalities with its high resolution and
21 lower patient exposure doses.^{1, 5, 14, 15} Moreover, CBCT can provide better diagnostics for the
22 bony changes in TMJ thanks to its higher resolution cross-sectional images and lower cost of
23 examination equipment and facility.¹² However, CBCT cannot provide any reliable
24 interpretation of soft tissues as it has lower image contrast compared to CT.¹ In addition to
25 those disadvantages, CBCT has higher image noise compared to CT.¹² Although sometimes it
26 is suggested to use a silicone index for the TMJ imaging by CBCT, a specific patient preparation
27 method is not obligatory.^{12, 16} A certain contraindication was not reported yet, which also makes
28 it a favorable imaging method for the bony structures of the TMJ.¹²

29 30 31 32 33 34 **1.3. Knowledge Among Dental Practitioners on Interpretation of CBCT**

35
36 As reported by EADMFR, the level of knowledge among dentists is not always sufficient to
37 interpret CBCT images, as dental schools may not provide enough lecturing for the
38 undergraduate students. Moreover, as dentomaxillofacial radiology post-graduate programs are
39 not common in most of the European countries, it may not be possible to consult 3D images
40 with dental radiology specialists (oral diagnosis and dentomaxillofacial radiology specialists).
41 As most of the CT and CBCT images demonstrate the bony structures of the TMJ in larger field
42 of view (FOV) values, the mandibular condylar process is a common anatomical structure on
43 those 3D images (**Basic training requirements for the use of dental CBCT by dentists: a
44 position paper prepared by the European Academy of Dentomaxillofacial Radiology.**<sup>2, 5,
45 7, 12</sup>

46 47 48 49 50 **1.4. Digital Imaging and Communications in Medicine and Standard Triangle Language**

51
52 DICOM (Digital Imaging and Communications in Medicine) and STL (Standard Triangle
53 Language) are two distinct data formats that are interacting as more and more of the dental field
54 advances into three-dimensional Understanding these standards' origins may be useful for
55 comprehending the functions they perform. The first data format is known as DICOM, as in.
56 This has been the norm for all medical digital radiography for many years. It not only covers
57 the formats to be used for digital medical image archiving, but it also includes the
58 communications protocols that are important for the process of diagnostic imaging. The
59
60
61
62
63
64
65

1 DICOM standard for digital radiographs was created primarily to maintain uniformity in image
2 file format. As DICOM protocol requirements are utilized when interacting with a Picture
3 Archiving and Communication System (PACS), it is far less practical for a regular dental clinic.
4 Larger centers (dentistry faculties, hospitals) that need to perform, store, and manage a variety
5 of digital radiography often integrate PACS. In a dental office, the traditional CBCT scans are
6 typically stored by the imaging software in DICOM format. The second data format that has
7 become more important to dentistry recently is STL, also known as stereolithography. This
8 format has its origins in the fields of 3D printing, computer-aided design, and computer-aided
9 manufacturing. It describes the surface geometry of a three-dimensional object and has become
10 the data format that most 3D printers and milling systems require. In a dental office, the
11 traditional intraoral scanner will output in STL format. While the DICOM approach to 3D
12 breaks the volume into slices, The STL format breaks the surface of the volume down into
13 "tiles," which are typically triangular. As a result, the DICOM file tends to provide more
14 information about what's inside the volume, while the STL file tends to provide more
15 information about the surface of the volume.^{15, 17, 18, 19, 20, 21, 22, 23, 24, 25}

19 **1.5. Deep Learning in Dentomaxillofacial Radiology**

21 Artificial intelligence (AI) is a term used to describe a computing system that mimics a natural
22 system. Deep learning (DL) techniques have recently been used for the analysis of medical
23 images, and they have demonstrated promise in a number of applications. Intelligent systems
24 have demonstrated value in predicting and identifying issues.^{26, 27} DL enables the application
25 of AI to common clinical issues across all dental departments. Software is being rapidly
26 enhanced to be the "person in charge" in the next few days as the accuracy of DL algorithms in
27 radiology and pathology keeps increasing with each upgrade.²⁸ Some of the use cases of DL in
28 the field of DMFR are prediction of oral cancer, evaluation of oral cancer risk, determination
29 of TMJ disorders progression, evaluation of conventional 2D images such as
30 orthopantomograms, periapical and bitewing radiographs, and evaluation of CBCT and other
31 3D images.^{28, 29, 30, 31}

32 The aim of this study is to assess the viability of the evaluation of the TMJ osseous degenerative
33 changes with AI-generated STL segmentations.

39 **2. Materials and methods**

41 The study protocol was approved by the Health Sciences Ethics Committee on July 28, 2022,
42 with the file number YDU/2022/105-1591. The Helsinki Declaration's guiding principles were
43 used in the investigation. Patients whose condylar process is within the field of view of a CBCT
44 scan were involved in the study. No specific clinical information was required.

45 A total of 432 anonymous retrospective CBCT images, which were acquired from 4 different
46 universities and from 4 different CBCT units, were evaluated in this study. Six
47 dentomaxillofacial radiologists evaluated the data in terms of flattening, erosion, osteophyte
48 formation, osteosclerosis, bifid condyle formation, and other conditions such as hyperplasia and
49 hypoplasia from anonymized DICOM files that were shared by each author in a cloud system.
50 Each radiologist evaluated the data separately and recorded their findings on a spreadsheet.

51 Flattening was evaluated as the absence (Grade 0) or presence (Grade 1) of flattening of the
52 condyle. Erosion was evaluated in 4 different grades as; absence of erosion (Grade 0), reduced
53 density that is localized only at cortical plates (Grade 1), presence of pitted and irregular
54
55
56
57
58
59
60
61
62
63
64
65

1 contours of the bone surfaces that extend into the superior layers of adjacent subcortical bone
2 (Grade 2), presence of pitted and irregular contours of the bone surfaces that extend to the
3 inferior portion of the superior layers of adjacent subcortical bone (Grade 3). Osteophyte
4 formation was evaluated in 4 different grades as; absence of osteophyte formation (Grade 0),
5 marginal bony prominence above the condyle that is shorter than 1mm (Grade 1), marginal
6 bony prominence above the condyle that is between 1-2 mms (Grade 2), marginal bony
7 prominence above the condyle that is longer than 2mms (Grade 3). Osteosclerosis was
8 evaluated in 2 different grades: absence (Grade 0) or presence (Grade 1) of osteosclerosis.
9

10 Following the end of the first evaluation stage, a consensus meeting was set in order to discuss
11 the differences in diagnosis. A ground truth was set as a result of the consensus meeting, and it
12 was recorded on a spreadsheet file by a separate observer, the ground truth observer (GT). STL
13 files were generated using a web-based dental AI software (**Diagnocat Inc., San Francisco,**
14 **CA, USA**), and the automatic segmentations of the mandibles were downloaded and re-
15 evaluated by two dentomaxillofacial radiologists to compare the ICC value between the GT and
16 STL examinations (**Figure 1**).
17
18
19

20 Comparison was made according to the hypothesis of whether the "average measures"
21 corresponding intraclass correlation coefficient (ICC) value is 0. If the obtained significance
22 value (p-value) is less than 0.05, the hypothesis is rejected, and it can be concluded that the ICC
23 value is significant. ICCs were classified as: 0.00-0.50: poor reliability, 0.50-0.75: moderate
24 reliability, 0.75-0.90: good reliability, and 0.90-1.00: excellent reliability.
25
26

27 3. RESULTS

28 3.1 First Evaluation Before the Consensus

29 The condyles of the temporomandibular joint were evaluated for five osseous changes, namely
30 flattening, erosion, osteophyte formation, osteosclerosis, and bifid condyle formation, by six
31 dentomaxillofacial radiologists. The interclass correlation (ICC) values for these changes
32 ranged from 0.927 to 0.971, indicating excellent reliability among the observers (Table 1). A
33 consensus meeting was held to review the diagnoses, and as a result, a ground truth (GT)
34 observer was generated.
35
36
37
38
39
40

41 Based on the ground truth observer's spreadsheet, out of 864 condyles, 372 cases of flattening,
42 185 cases of erosion, 70 cases of osteophyte formation, 117 cases of osteosclerosis, and 15 cases
43 of bifid condyle formation were identified. When comparing the diagnoses based on the
44 examination of STL files to those of the ground truth observer, the interclass correlation (ICC)
45 values for flattening, erosion, osteophyte formation, osteosclerosis, and bifid condyle formation
46 were 1.000, 0.782, 1.000, 0.000, and 1.000, respectively.
47
48

49 4. DISCUSSION

50 Applications for computer-aided design (CAD) and 3D printing can utilize STL files. CBCT
51 scans can provide STL files that can be used to make 3D models of the TMJ in dentistry. The
52 visualization of the joint's anatomy and the detection of any anomalies can both benefit from
53 the usage of STL files in the diagnosis of TMJ diseases. The following are some particular ways
54 in which STL files might assist with the identification of TMJ issues on computed tomography
55 scans: 1, 5, 15, 19, 22, 23, 32, 33, 34, 35, 36, 37
56
57
58
59
60
61
62
63
64
65

- Visualization of bony structures: STL files allow clinicians to view the bony structures of the TMJ in 3D, which can provide greater detail than 2D CT scans alone. This can aid in the identification of bony abnormalities such as condylar hyperplasia, erosion, or osteoarthritis.
- Assessment of joint space: STL files can be used to measure the distance between the condyle and fossa, which can aid in the diagnosis of disc displacement or joint space narrowing.
- Evaluation of condylar position: STL files can help assess the position of the condyle in relation to the fossa, which can aid in the diagnosis of condylar displacement or subluxation.
- Planning of surgical or non-surgical interventions: STL files can be utilized to plan TMJ surgery or non-surgical therapies. For instance, a surgical guide 3D-printed from an STL file can help with the accurate implantation of orthopedic implants during TMJ surgery.

STL files generated from cone beam computed tomography (CBCT) scans can provide a 3D model of the TMJ, allowing for a comprehensive evaluation of bony structures, including the mandibular condyle, glenoid fossa, and articular eminence. Compared to traditional 2D imaging methods, such as panoramic and lateral cephalometric radiographs, CBCT scans and STL files provide more accurate and detailed information about the complex bony anatomy of the TMJ. However, it is important to note that the quality of the CBCT scan and the expertise of the operator in generating the STL files can greatly affect the accuracy and precision of the resulting 3D model. Additionally, STL files do not provide information on the soft tissue structures of the TMJ, such as the articular disc, which is important in the diagnosis and treatment of TMJ disorders. Therefore, while STL files can be a valuable tool in evaluating the bony features of the TMJ, they should be used in conjunction with other imaging methods and clinical findings to provide a comprehensive evaluation and diagnosis of TMJ disorders.^{1, 5, 15, 19, 22, 23, 32, 33, 34, 36, 37, 38}

The results of this study also reported perfect success for the bifid condyle formation, osteophyte formation, and flattening; however, the ICC values for the erosion and osteosclerosis were 0.782 and 0.000, respectively. As the STL files that were generated by the AI software we used were unable to differentiate the cortical borders from the trabecular bone, the dentomaxillofacial radiologists who evaluated the STL files were unable to detect grade 1 erosions. It is fair to state that advanced erosions are demonstrative in STL files, but the diagnosis of the initial erosions requires exact visualization of the cortical borders. Moreover, the specialists were unable to detect osteosclerosis of the trabecular bone of the condylar process in STL files, as the STL files only demonstrated the superficial formation. In this study, none of the osteosclerotic condyles could be diagnosed in STL files.

In their study, Kamio et al.²³ assessed the efficacy of nine different software programs for generating STL models from MDCT DICOM files. The researchers utilized a dry human mandible with two 10-mm-diameter bearing balls during the scanning process. The results indicated that there were variations in file size and the number of triangles comprising each STL model across all software packages, but there were no statistically significant differences observed. The mean shape error for the mandibular STL model was 0.11 mm, and there was no significant variation between the software packages. The authors emphasized the importance of understanding the features of each software package, particularly in the fine and thin regions of the osseous structures, despite the observed differences in performance.

1 There were five major limitations for this study. As all of the STL files were generated
2 from a single CBCT device and a single AI-software, this study cannot state whether the results
3 will be the same for all other CBCT devices and softwares. For a better generalizability study
4 should be done with multiple CBCT devices and multiple softwares since Kamio et al.²³
5 reported that differences exist depending on the STL segmentation of the software. Also, STL
6 files do not provide information on the soft tissue structures of the TMJ, such as the articular
7 disc; thus, this study does not cover all of the diagnoses of the TMJ disorders. Moreover, As
8 STL files can only represent the outer features of a structure any evaluation that requires the
9 differentiation of the trabecular and cortical bone may not be done with this technique. The
10 study may not compare the accuracy of the AI-generated STL files with other imaging
11 modalities, such as MDCT or MRI scans, which can limit the understanding of the overall
12 accuracy and usefulness of STL files for TMJ diagnosis.
13
14

15 **5. CONCLUSION**

16
17
18 TMJ evaluation of the AI-generated STL files were perfect for bifid condyle formation,
19 osteophyte formation, and flattening; however, osteosclerosis could not be diagnosed just by
20 using AI-generated STL files. The grade of erosion was a determining factor in the diagnoses,
21 as Grade 1 erosions could not be diagnosed on STL files as the cortical bone and trabecular
22 bone were inseparable from each other.
23
24
25
26
27
28
29
30
31
32
33
34
35
36
37
38
39
40
41
42
43
44
45
46
47
48
49
50
51
52
53
54
55
56
57
58
59
60
61
62
63
64
65

REFERENCES

1. Wang YH, Ma RH, Li JJ, Mu CC, Zhao YP, Meng JH, et al. Diagnostic efficacy of CBCT, MRI and CBCT-MRI fused images in determining anterior disc displacement and bone changes of temporomandibular joint. *Dentomaxillofac Radiol.* 2022;51(2):20210286.
2. Ocak M, Sargon MF, Orhan K, Bilecenoglu B, Geneci F, Uzun MB. Evaluation of the anatomical measurements of the temporomandibular joint by cone-beam computed tomography. *Folia Morphol (Warsz).* 2019;78(1):174-81.
3. Meral SE, Karaaslan S, Tuz HH, Uysal S. Evaluation of the temporomandibular joint morphology and condylar position with cone-beam computerized tomography in patients with internal derangement. *Oral Radiol.* 2022.
4. Orhan K, Nishiyama H, Tadashi S, Shumei M, Furukawa S. MR of 2270 TMJs: prevalence of radiographic presence of otomastoiditis in temporomandibular joint disorders. *Eur J Radiol.* 2005;55(1):102-7.
5. Kurt H, Orhan K, Aksoy S, Kursun S, Akbulut N, Bilecenoglu B. Evaluation of the superior semicircular canal morphology using cone beam computed tomography: a possible correlation for temporomandibular joint symptoms. *Oral Surg Oral Med Oral Pathol Oral Radiol.* 2014;117(3):e280-8.
6. Orhan K, Delilbasi C, Paksoy C. Magnetic resonance imaging evaluation of mandibular condyle bone marrow and temporomandibular joint disc signal intensity in anaemia patients. *Dentomaxillofac Radiol.* 2009;38(5):247-54.
7. Verhelst PJ, Vervaeke K, Orhan K, Lund B, Benchimol D, Coucke W, et al. The agreement between magnetic resonance imaging and arthroscopic findings in temporomandibular joint disorders. *Int J Oral Maxillofac Surg.* 2021;50(5):657-64.
8. Akkemik O, Kugel H, Fischbach R. Acute soft tissue injury to the temporomandibular joint and posttraumatic assessment after mandibular condyle fractures: a longitudinal prospective MRI study. *Dentomaxillofac Radiol.* 2022;51(3):20210148.
9. Lin B, Cheng M, Wang S, Li F, Zhou Q. Automatic detection of anteriorly displaced temporomandibular joint discs on magnetic resonance images using a deep learning algorithm. *Dentomaxillofac Radiol.* 2022;51(3):20210341.
10. Luo D, Qiu C, Zhou R, Yu W, Li X, Yang J. MRI-based observation of the size and morphology of temporomandibular joint articular disc and condyle in young asymptomatic adults. *Dentomaxillofac Radiol.* 2022;51(3):20210272.
11. Nozawa M, Ito H, Arijji Y, Fukuda M, Igarashi C, Nishiyama M, et al. Automatic segmentation of the temporomandibular joint disc on magnetic resonance images using a deep learning technique. *Dentomaxillofac Radiol.* 2022;51(1):20210185.
12. Rozylo-Kalinowska I, Orhan K. *Imaging of the Temporomandibular Joint*: Springer Nature; 2019. 406 p.
13. Hintze H, Wiese M, Wenzel A. Cone beam CT and conventional tomography for the detection of morphological temporomandibular joint changes. *Dentomaxillofac Radiol.* 2007;36(4):192-7.
14. Guidelines on CBCT for Dental and Maxillofacial Radiology 2012 [Available from: <https://www.sedentext.eu/>].
15. Huotilainen E, Jaanimets R, Valasek J, Marcian P, Salmi M, Tuomi J, et al. Inaccuracies in additive manufactured medical skull models caused by the DICOM to STL conversion process. *J Craniomaxillofac Surg.* 2014;42(5):e259-65.
16. Szopinski K, Regulski PA. A simple graded bite block for dynamic magnetic resonance imaging of the temporomandibular joint. *Dentomaxillofac Radiol.* 2022;51(1):20210119.

17. Alhossaini SJ, Neena AF, Issa NO, Abouelkheir HM, Gaweesh YY. Accuracy of markerless registration methods of DICOM and STL files used for computerized surgical guides in mandibles with metal restorations: An in vitro study. *J Prosthet Dent.* 2022.
18. Cai T, Rybicki FJ, Giannopoulos AA, Schultz K, Kumamaru KK, Liacouras P, et al. The residual STL volume as a metric to evaluate accuracy and reproducibility of anatomic models for 3D printing: application in the validation of 3D-printable models of maxillofacial bone from reduced radiation dose CT images. *3D Print Med.* 2015;1(1):2.
19. D'Addazio G, Xhajanka E, Traini T, Santilli M, Rexhepi I, Murmura G, et al. Accuracy of DICOM-DICOM vs. DICOM-STL Protocols in Computer-Guided Surgery: A Human Clinical Study. *J Clin Med.* 2022;11(9).
20. Hwang JJ, Jung YH, Cho BH. The need for DICOM encapsulation of 3D scanning STL data. *Imaging Sci Dent.* 2018;48(4):301-2.
21. Jonske F, Dederichs M, Kim MS, Keyl J, Egger J, Umutlu L, et al. Deep Learning-driven classification of external DICOM studies for PACS archiving. *Eur Radiol.* 2022;32(12):8769-76.
22. Kamio T, Kawai T. CBCT Images to an STL Model: Exploring the "Critical Factors" to Binarization Thresholds in STL Data Creation. *Diagnostics (Basel).* 2023;13(5).
23. Kamio T, Suzuki M, Asami R, Kawai T. DICOM segmentation and STL creation for 3D printing: a process and software package comparison for osseous anatomy. *3D Print Med.* 2020;6(1):17.
24. Long Z, Walz-Flannigan AI, Littrell LA, Schueler BA. Technical note: Four-year experience with utilization of DICOM metadata analytics in clinical digital radiography practice. *Med Phys.* 2023;50(2):831-6.
25. Muller H, Fossey A. Stereolithography (STL) measurement rubric for the evaluation of craniomaxillofacial STLs. *3D Print Med.* 2022;8(1):25.
26. Buyuk C, Akkaya N, Arsan B, Unsal G, Aksoy S, Orhan K. A Fused Deep Learning Architecture for the Detection of the Relationship between the Mandibular Third Molar and the Mandibular Canal. *Diagnostics (Basel).* 2022;12(8).
27. Radwan MT, Sin C, Akkaya N, Vahdettin L. Artificial intelligence-based algorithm for cervical vertebrae maturation stage assessment. *Orthod Craniofac Res.* 2022.
28. Ünsal G, Orhan K. Deep Learning and Artificial Intelligence Applications in Dentomaxillofacial Radiology. In: Ozsahin I, Uzun-Ozsahin D, editors. *Applied Machine Learning and Multi-Criteria*; Bentham Science Publishers; 2021. p. 126-40.
29. Feher B, Kuchler U, Schwendicke F, Schneider L, Cejudo Grano de Oro JE, Xi T, et al. Emulating Clinical Diagnostic Reasoning for Jaw Cysts with Machine Learning. *Diagnostics (Basel).* 2022;12(8).
30. Mohammad-Rahimi H, Motamedian SR, Pirayesh Z, Haiat A, Zahedrozegar S, Mahmoudinia E, et al. Deep learning in periodontology and oral implantology: A scoping review. *J Periodontal Res.* 2022;57(5):942-51.
31. Schwendicke F, Cejudo Grano de Oro J, Garcia Cantu A, Meyer-Lueckel H, Chaurasia A, Krois J. Artificial Intelligence for Caries Detection: Value of Data and Information. *J Dent Res.* 2022;101(11):1350-6.
32. Borohovitz CL, Abraham Z, Redmond WR. The diagnostic advantage of a CBCT-derived segmented STL rendition of the teeth and jaws using an AI algorithm. *J Clin Orthod.* 2021;55(6):361-9.
33. Chen H, van Eijnatten M, Aarab G, Forouzanfar T, de Lange J, van der Stelt P, et al. Accuracy of MDCT and CBCT in three-dimensional evaluation of the oropharynx morphology. *Eur J Orthod.* 2018;40(1):58-64.
34. Choi E, Kim D, Lee JY, Park HK. Artificial intelligence in detecting temporomandibular joint osteoarthritis on orthopantomogram. *Sci Rep.* 2021;11(1):10246.

- 1
2
3
4
5
6
7
8
9
10
11
12
13
14
15
16
17
18
19
20
21
22
23
24
25
26
27
28
29
30
31
32
33
34
35
36
37
38
39
40
41
42
43
44
45
46
47
48
49
50
51
52
53
54
55
56
57
58
59
60
61
62
63
64
65
35. Mankowski J, Piekos J, Dominiak K, Klukowski P, Fotek M, Zawisza M, et al. A Mandible with the Temporomandibular Joint-A New FEM Model Dedicated to Strength and Fatigue Calculations of Bonding Elements Used in Fracture and Defect Surgery. *Materials (Basel)*. 2021;14(17).
 36. Aksoy S, Kelahmet U, Hincal E, Oz U, Orhan K. Comparison of linear and angular measurements in CBCT scans using 2D and 3D rendering software. *Biotechnology & Biotechnological Equipment*. 2016;30(4):777-84.
 37. Shahbazian M, Jacobs R, Wyatt J, Willems G, Pattijn V, Dhoore E, et al. Accuracy and surgical feasibility of a CBCT-based stereolithographic surgical guide aiding autotransplantation of teeth: in vitro validation. *J Oral Rehabil*. 2010;37(11):854-9.
 38. Son DM, Yoon YA, Kwon HJ, An CH, Lee SH. Automatic Detection of Mandibular Fractures in Panoramic Radiographs Using Deep Learning. *Diagnostics (Basel)*. 2021;11(6).

Figure Legends

Figure 1: STL files of a healthy case with erosion, flattening, bifid condyle formation, and osteophyte formation greater than 2mm.

Table Legends

Table 1: ICC values of the 6 dentomaxillofacial radiologists

**Evaluation of Temporomandibular Joint Osseous Degenerative Changes with Artificial Intelligence
Generated STL Segmentations**

**Kaan Orhan^{1,*}, Alex Sanders², Gürkan Ünsal³, Matvey Ezhov², Melis Mısırlı⁴, Maxim Gusarev², Murat İçen⁵,
Mamat Shamshiev², Gave Keser⁶, Maria Golitsyna², Merve Onder¹, David Manulis², Cemal Atakan⁷**

1-) Ankara University, Faculty of Dentistry, Department of Dentomaxillofacial Radiology, Ankara, TR

2) Diagnostics Inc, California, US

3-) Near East University, Faculty of Dentistry, Department of Dentomaxillofacial Radiology, Nicosia, CY

4-) International Final University, Faculty of Dentistry, Department of Dentomaxillofacial Radiology, Nicosia, CY

5-) Nevşehir Hacı Bektaş Veli University, Faculty of Dentistry, Department of Dentomaxillofacial Radiology,
Nevşehir, TR

6-) Marmara University, Faculty of Dentistry, Department of Dentomaxillofacial Radiology, Istanbul, TR

7-) Ankara University, Faculty of Science and Letters, Department of Statistics, Ankara, TR

***Corresponding Author:** Prof. Dr. Kaan ORHAN

Ankara University, Faculty of Dentistry, Department of Dentomaxillofacial Radiology, **Besevler/Ankara/TR**

e-mail: call53@yahoo.com, **Telephone Number:** +90 5356765010

Conflict of interest statement: All authors declare that they have no conflict of interest.

Funding: This research did not receive any specific grant from funding agencies in the public, commercial, or not-for-profit sectors.

Human rights statements and informed consent: All applicable international, national, and/or institutional guidelines for the care and use of animals were followed. All procedures performed in studies involving human participants were in accordance with the ethical standards of the institutional and/or national research committee and with the 1964 Helsinki declaration and its later amendments or comparable ethical standards. This study was found ethically appropriate at the meeting of Near East University IRB. Informed consent was obtained from all individual participants included in the study.

Author Contributions

K.O.: Conceptualization, study design, critical review, editing, draft of the paper

G.Ü.: Data selection, contributed data, or analysis tools, draft of the paper, statistical Analysis

M.M.: Data selection, contributed data, or analysis tools

A.S., M.E., D.M., M.G., G.K., M.O., M.S.: Data selection, contributed data, or analysis tools

C.A.: Statistical Analysis

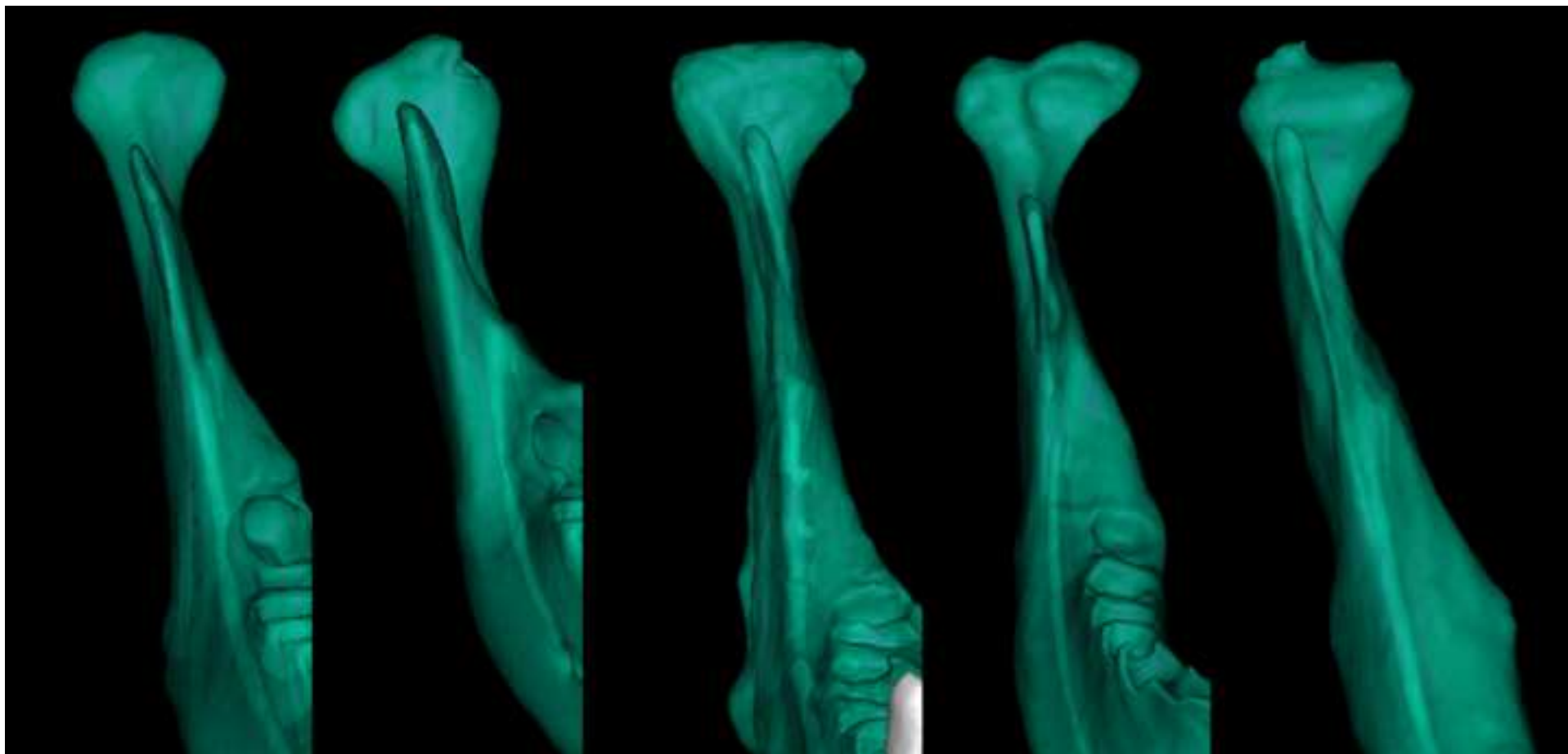


Table 1

Intraclass Correlation Coefficient for Osteophyte Formation							
	Intraclass Correlation	95% Confidence Interval		F Test with True Value 0			
		Lower Bound	Upper Bound	Value	df1	df2	Sig
Single Measures	,708	,676	,739	17,979	862	5172	,000
Average Measures	,944	,936	,952	17,979	862	5172	,000*
Intraclass Correlation Coefficient for Erosion							
	Intraclass Correlation	95% Confidence Interval		F Test with True Value 0			
		Lower Bound	Upper Bound	Value	df1	df2	Sig
Single Measures	,810	,787	,832	30,856	862	5172	,000
Average Measures	,968	,963	,972	30,856	862	5172	,000*
Intraclass Correlation Coefficient for Flattening							
	Intraclass Correlation	95% Confidence Interval		F Test with True Value 0			
		Lower Bound	Upper Bound	Value	df1	df2	Sig
Single Measures	,818	,795	,839	32,431	862	5172	,000
Average Measures	,969	,965	,973	32,431	862	5172	,000*
Intraclass Correlation Coefficient for Bifid Condyle Formation							
	Intraclass Correlation	95% Confidence Interval		F Test with True Value 0			
		Lower Bound	Upper Bound	Value	df1	df2	Sig
Single Measures	,825	,803	,846	30,856	862	5172	,000
Average Measures	,971	,966	,975	30,856	862	5172	,000*
Intraclass Correlation Coefficient for Osteosclerosis							
	Intraclass Correlation	95% Confidence Interval		F Test with True Value 0			
		Lower Bound	Upper Bound	Value	df1	df2	Sig

Single Measures	,644	,608	,679	13,650	862	5172	,000
Average Measures	,927	,916	,937	13,650	862	5172	,000*